

Alma Mater Studiorum Università di Bologna
Archivio istituzionale della ricerca

A new hemodynamic model for the study of cerebral venous outflow

This is the final peer-reviewed author's accepted manuscript (postprint) of the following publication:

Published Version:

Gadda, G., Taibi, A., Sisini, F., Gambaccini, .M., Zamboni, .P., Ursino, M. (2015). A new hemodynamic model for the study of cerebral venous outflow. AMERICAN JOURNAL OF PHYSIOLOGY. HEART AND CIRCULATORY PHYSIOLOGY, 308(3), H217-H231 [10.1152/ajpheart.00469.2014].

Availability:

This version is available at: <https://hdl.handle.net/11585/522980> since: 2015-12-07

Published:

DOI: <http://doi.org/10.1152/ajpheart.00469.2014>

Terms of use:

Some rights reserved. The terms and conditions for the reuse of this version of the manuscript are specified in the publishing policy. For all terms of use and more information see the publisher's website.

This item was downloaded from IRIS Università di Bologna (<https://cris.unibo.it/>).
When citing, please refer to the published version.

(Article begins on next page)

This is the final peer-reviewed accepted manuscript of:

A new hemodynamic model for the study of cerebral venous outflow

G. Gadda, A. Taibi, F. Sisini, M. Gambaccini, P. Zamboni, and M. Ursino

American Journal of Physiology-Heart and Circulatory Physiology 2015 308:3, H217-H231

The final published version is available online at:

<https://doi.org/10.1152/ajpheart.00469.2014>

Rights / License:

The terms and conditions for the reuse of this version of the manuscript are specified in the publishing policy. For all terms of use and more information see the publisher's website.

This item was downloaded from IRIS Università di Bologna (<https://cris.unibo.it/>)

When citing, please refer to the published version.

1 **Title Page**

2 **Title**

3 A new hemodynamic model for the study of cerebral venous outflow

4 **Authors**

5 Gadda G.¹, Taibi A.¹, Sisini F.¹, Gambaccini M.¹, Zamboni P.², Ursino M.³

6

7 **Affiliation**

8 ¹ Department of Physics and Earth Sciences, University of Ferrara, Ferrara, Italy.

9 ² Vascular Diseases Center, University of Ferrara, Cona, FE, Italy.

10 ³ Department of Electrical, Electronic and Information Engineering, University of
11 Bologna, Bologna, Italy.

12

13 **Running Head**

14 Hemodynamic model of the cerebral venous outflow

15 **Address for Correspondence**

16 Giacomo Gadda

17 Department of Physics and Earth Sciences,

18 University of Ferrara,

19 Via Saragat 1, 44122, Ferrara, Italy.

20 Email: giacomo.gadda@student.unife.it

21 **Abstract**

22 We developed a mathematical model of the cerebral venous outflow for the simulation
23 of the average blood flows and pressures in the main drainage vessels of the brain. The
24 main features of the model are that it includes a validated model for the simulation of
25 the intracranial circulation, and it accounts for the dependence of the hydraulic proper-
26 ties of the jugular veins with respect to the gravity field. That makes it an useful tool for
27 the study of the correlations between extracranial blood redistributions and changes in
28 the intracranial environment. The model is able to: simulate the average pressures and
29 flows in different points of the jugular ducts, taking into account the amount of blood
30 coming from the anastomotic connections; simulate how the blood redistribution due to
31 change of posture affects flows and pressures in specific points of the system; simulate
32 redistributions due to stenotic patterns. Sensitivity analysis to check the robustness of
33 the model were performed. The model reproduces average physiologic behavior of the
34 jugular, vertebral, and cerebral ducts in terms of pressures and flows. In fact, jugular
35 flow drops from about 11.7 ml/s to about 1.4 ml/s in the passage from supine to stand-
36 ing. At the same time, vertebral flow increases from 0.8 to 3.4 ml/s, while cerebral
37 blood flow, venous sinuses pressure and intracranial pressure are constant around the
38 average value of 12.5 ml/s, 6 mmHg and 10 mmHg, respectively. All these values are
39 in agreement with literature data.

40 **Keywords**

41 cerebral outflow, mathematical modeling.

42 **Main Text**

43 **Introduction**

44 The extracranial venous system represents an important determinant of the brain cir-
45 culation, but its role in the pathology of the central nervous system is not fully under-
46 stood yet [4] [24]. It is recognized that, in supine position, the jugular veins represent
47 the main outflow route for the cerebral circulation [2] [5] [23] [33] [36], being able to
48 carry most of blood flow from the brain and from other extracerebral territories (ap-
49 proximately 700-720 ml/min [25] [31]) with respect to a cerebral blood inflow of about
50 750 ml/min [43]. However, the jugular venous system exhibits important flow limi-
51 tation during upright posture changes, because the jugular veins tend to collapse as a
52 consequence of the decrease of transmural pressure due to the gravitational field, caus-
53 ing a significant increase in resistance [3] [6] [11] [13] [24]. In the absence of other
54 routes for extracranial outflow, this flow limitation would have dramatic effects on the
55 cerebral circulation, since, apart from brief transient time intervals, the average cranial
56 arterial inflow is expected to be equal to the cranial venous outflow for the mass con-
57 servation.

58 As a consequence, large attention has been devoted to the venous circulation in upright
59 state, in an effort to understand which alternative routes can carry the brain venous
60 outflow. It has long been postulated that the vertebral venous system may provide an
61 important alternative route for venous outflow when standing or sitting; this was first
62 demonstrated with the use of contrast media in rhesus monkeys [8] and subsequently
63 measured in humans with the Doppler and magnetic resonance imaging technique [2]
64 [5] [6] [23] [36]. Valdueza et al. [31] observed that blood flow in the jugular veins de-
65 creases from 700 ml/min in supine position down to 70 ml/min at 90° elevation, while
66 blood flow in the vertebral veins raises from 40 to 210 ml/min.

67 Accordingly, a classical model of the cerebral venous outflow assumes the existence of
68 two main alternative routes: a route through the jugular veins, with smaller resistance
69 in supine conditions, and a parallel vertebral route with higher resistance. In upright

70 conditions, when the first route collapses, blood flow is diverted to the second one.
 71 Based on this idea, Gisolf et al [13] developed a mathematical model of cerebral ve-
 72 nous outflow: the model consists of two jugular veins (each composed of a chain of 10
 73 units with resistances and capacitances) and a vertebral plexus (described with a single
 74 resistance). The elements in the jugular veins collapse according to the "tube law" [3]
 75 [11] during a posture change, but can reopen during a Valsalva maneuver. With this
 76 model, the authors studied how venous blood flow changes from the supine to the up-
 77 right position, and confirmed that the cerebral venous distribution depends on posture.
 78 Despite the previous pivotal studies, many aspects of the cerebral venous outflow sys-
 79 tem are still problematic.
 80 First, it is well-known that cerebral autoregulation maintains blood flow to the brain
 81 quite constant, despite pressure changes [1] [19]: this signifies that an amount of blood
 82 flow much greater than that measured in the vertebral system must be carried out in
 83 the upright state. This discrepancy was clearly recognized by Valdueza et al. [31] who
 84 observed that "a main difference of about 450 ml/min remained". These authors hy-
 85 pothesized that other routes, such as the epidural veins, significantly contribute to the
 86 orthostatic venous outflow.
 87 Second, some authors, using the color Doppler technique, recently observed that blood
 88 flow along the jugular veins in upright conditions is not longitudinally constant, but
 89 increases progressively when the measurement site is moved from the upright sections
 90 (close to the jugular foramen into the skull) to the downstream sections (close to the
 91 subclavian vein) [5] [26] [39] [42]. This observation supports the idea that additional
 92 anastomotal routes carry part of the cranial blood flow to the jugular veins even in
 93 the upright position, bypassing the upstream more collapsed sections. In fact, as a
 94 consequence of the different effect of gravity, only the higher portions of the jugular
 95 veins are probably fully collapsed, whereas the downstream sections are opened. A
 96 comprehensive model of the cerebral venous outflow should also include these further
 97 collateral routes.
 98 Due to the complexity of the relationships involved, and the large variability in the

99 anatomical parameters, it is extremely difficult to understand the effect of alterations
100 in the extracranial venous circulation in simple qualitative terms. The study of the
101 cerebral venous outflow, and of its implications in healthy and diseased conditions, can
102 largely benefit from the use of computational models.

103 So far, most models of the cerebral circulation focused on the intracranial circula-
104 tion and on its control mechanisms, by providing just a very simplified description
105 of extracranial venous return. A notable exception is the model by Gisolf et al. [13]
106 mentioned above, which, however, includes only the vertebral plexus as an alternative
107 drainage pathway.

108 The aim of the present study is to develop and validate a comprehensive original
109 lumped parameter model of the cerebral venous outflow system, which overcomes
110 some of the limitations noticed above. In particular, compared with the model by
111 Gisolf et al. [13] the present model also includes:

- 112 • an accurate model of the intracranial circulation developed in past years, which
113 incorporates the autoregulation of cerebral blood flow [12] [29] [30]. This model
114 furnishes the correct values of cerebral blood flow to the venous return model.
115 Moreover, it allows a quantitative analysis of the effect of alterations in the ve-
116 nous pathways on intracranial quantities, such as the effect on intracranial pres-
117 sure, venous sinuses pressure, capillary pressure and cerebrospinal fluid circula-
118 tion
- 119 • a more sophisticated description of the collateral pathways, including not only
120 the vertebral plexus, but also other anastomoses leading blood to the downstream
121 sections of the jugular veins [5] [39] [42].

122 In the following, the model is described qualitatively, with emphasis on the new
123 aspects, and parameters are given in accordance with the physiology. All equations are
124 presented in Appendix. The model is validated against results in the literature, con-
125 cerning the effect of a posture change in healthy subjects; a sensitivity analysis is also
126 performed to clarify the role of the alterations in some parameters.

127 The model may represent an useful tool for the study of the correlation between pos-
 128 ture variations, vessel conductances (normal or abnormal) and the consequent pressure
 129 and flow changes. This may have a great impact toward a deeper understanding of
 130 pathological disorders involving abnormalities of the cerebral venous outflow. In per-
 131 spective, it may be used to assess which alterations in the extracranial venous outflow
 132 may be in relation with central nervous system disorders and aging [5] [9] [22] [38]
 133 [40].

134 Glossary

135 *A*

136 Parameter related to the resistance of the jugular segments to collapse

137 *AZY*

138 Lumbo-azygos system

139 *azy1*

140 Distal azygos

141 *azy2*

142 Proximal azygos

143 b_{CO_2}

144 Parameter related to CO_2 reactivity

145 *c3*

146 Upper segment of the collateral network

147 *cj2*

148 Lower anastomoses

149 *cj3*

150 Upper anastomoses

151 C_{azy}

152 Capacity of the azygos system

153 C_{c2}

154 Capacity of the middle segment of the collateral network

155

156 C_{c3}

157 Capacity of the upper segment of the collateral network

158 C_{ic}

159 Intracranial capacity

160 C_{jl2}

161 Capacity of the middle segment of the left jugular vein

162 C_{jl3}

163 Capacity of the upper segment of the left jugular vein

164 C_{jr2}

165 Capacity of the middle segment of the right jugular vein

166 C_{jr3}

167 Capacity of the upper segment of the right jugular vein

168 C_{pa}

169 Capacity of the pial arterioles

170 C_{pa_n}

171 Basal capacity of the pial arterioles

172 CSF

173 Cerebrospinal fluid

174 C_{svc}

175 Capacity of the superior vena cava

176 C_{vi}

177 Capacity of the intracranial veins

178 C_{vs}

179 Capacity of the terminal intracranial veins

180 C_{vv}

181 Capacity of the vertebral veins

182 C_x

183	Capacity of the generic segment x
184	
185	$\Delta_{C_{pa}}$
186	Amplitude of the curve of the pial arterioles capacity
187	$\Delta_{C_{pa1}}$
188	Value of the capacity of the pial arterioles during vasodilation simulation
189	$\Delta_{C_{pa2}}$
190	Value of the capacity of the pial arterioles during vasoconstriction simulation
191	g
192	Gravity acceleration
193	G_0
194	Conductance of the cerebrospinal fluid outflow tract
195	G_{aut}
196	Gain of the autoregulation mechanism related to cerebral blood flow variations
197	G_{azy1}
198	Conductance of the distal azygos
199	G_{azy2}
200	Conductance of the proximal azygos
201	G_{c1}
202	Conductance of the lower segment of the collateral network
203	G_{c2}
204	Conductance of the middle segment of the collateral network
205	G_{c3}
206	Conductance of the upper segment of the collateral network
207	G_{cjl2}
208	Conductance of the lower anastomotic connection (left side)
209	G_{cjl3}
210	Conductance of the upper anastomotic connection (left side)
211	G_{cjr2}

212	Conductance of the lower anastomotic connection (right side)
213	
214	G_{cjr3}
215	Conductance of the upper anastomotic connection (right side)
216	G_{CO_2}
217	Gain related to CO_2 reactivity
218	G_{ex}
219	Conductance of the external carotid arteries
220	G_{jl1}
221	Conductance of the lower segment of the left jugular vein
222	G_{jl2}
223	Conductance of the middle segment of the left jugular vein
224	G_{jl3}
225	Conductance of the upper segment of the left jugular vein
226	G_{jr1}
227	Conductance of the lower segment of the right jugular vein
228	G_{jr2}
229	Conductance of the middle segment of the right jugular vein
230	G_{jr3}
231	Conductance of the upper segment of the right jugular vein
232	G_{lv}
233	Conductance of the lumbar vein
234	G_{svc1}
235	Conductance of the upper segment of the superior vena cava (jugular confluence)
236	G_{svc2}
237	Conductance of the lower segment of the superior vena cava
238	G_{vs}
239	Conductance of the terminal intracranial veins
240	G_{vv2}

241	Conductance of the lower part of the vertebral vein
242	
243	G_{vvl1}
244	Conductance of the left vertebral vein
245	G_{vvr1}
246	Conductance of the right vertebral vein
247	G_x
248	Conductance of the generic segment x of the circulatory system
249	h
250	Length of a jugular segment
251	hbf
252	Mock cerebrospinal fluid possibly injected into or subtracted from the cranial cavity
253	IJV
254	Internal jugular vein
255	$J1$
256	Lower segment of the internal jugular veins
257	$J2$
258	Middle segment of the internal jugular veins
259	$J3$
260	Upper segment of the internal jugular veins
261	$jr3$
262	Upper segment of the right jugular vein
263	k_{CO_2}
264	Parameter related to CO_2 reactivity
265	$k_{C_{pa}}$
266	Parameter related to capacity of the pial arterioles
267	k_E
268	Intracranial elastance coefficient
269	k_{jl1}

270	Parameter related to basal conductance of the lower segment of the left jugular vein
271	
272	k_{jr1}
273	Parameter related to basal conductance of the lower segment of the right jugular vein
274	k_{jl2}
275	Parameter related to basal conductance of the middle segment of the left jugular vein
276	k_{jr2}
277	Parameter related to basal conductance of the middle segment of the right jugular vein
278	k_{jl3}
279	Parameter related to basal conductance of the upper segment of the left jugular vein
280	k_{jr3}
281	Parameter related to basal conductance of the upper segment of the right jugular vein
282	k_R
283	Parameter related to resistance of pial arterioles
284	k_{ven}
285	Parameter related to intracranial venous capacity
286	k_x
287	Parameter related to basal conductance of jugular and vertebral veins
288	pa
289	Pial arterioles
290	P_a
291	Arterial pressure
292	P_{aCO_2}
293	Partial pressure of carbon dioxide
294	P_{aCO_2n}
295	Basal partial pressure of carbon dioxide
296	P_{azy}
297	Pressure inside the azygos system
298	P_c

299	Pressure inside the intracranial capillaries
300	
301	P_{c2}
302	Pressure inside the middle segment of the collateral network
303	P_{c3}
304	Pressure inside the upper segment of the collateral network
305	P_{cv}
306	Pressure inside the vena cava
307	P_{ic}
308	Intracranial pressure
309	P_{icn}
310	Basal intracranial pressure
311	P_{j1ext}
312	Pressure outside the lower segment of the jugular veins
313	P_{j2ext}
314	Pressure outside the middle segment of the jugular veins
315	P_{j3ext}
316	Pressure outside the upper segment of the jugular veins
317	P_{jl2}
318	Pressure inside the middle segment of the left jugular vein
319	P_{jl3}
320	Pressure inside the upper segment of the left jugular vein
321	P_{jr2}
322	Pressure inside the middle segment of the right jugular vein
323	P_{jr3}
324	Pressure inside the upper segment of the right jugular vein
325	P_{lv}
326	Pressure inside the lumbar vein
327	P_{pa}

328 Pressure inside the pial arterioles
329
330 P_{svc}
331 Pressure in the lower segment of the superior vena cava
332 P_{svc1}
333 Pressure in the upper segment of the superior vena cava (jugular confluence)
334 P_v
335 Pressure inside the cerebral veins
336 P_{v1}
337 Transmural pressure value at which cerebral veins collapse
338 P_{vs}
339 Pressure inside the venous sinuses
340 P_{vv}
341 Pressure inside the vertebral veins
342 P_x
343 Pressure inside the generic segment x
344 P_{xext}
345 External pressure of the x segment of the internal jugular veins
346 P_{xint}
347 Internal pressure of the x segment of the internal jugular veins
348 Q
349 Cerebral blood flow
350 Q_0
351 Cerebrospinal fluid outflow rate
352 Q_{c3}
353 Flow in the upper segment of the collateral network
354 Q_{ex}
355 Flow in the external carotid arteries (flow to face and neck)
356 Q_f

357	Cerebrospinal fluid formation rate
358	
359	Q_{j1}
360	Total flow in the lower segments of the jugular veins
361	Q_{j2}
362	Total flow in the middle segments of the jugular veins
363	Q_{j3}
364	Total flow in the upper segments of the jugular veins
365	Q_{jr3}
366	Flow in the upper segment of the right jugular vein
367	Q_n
368	Basal cerebral blood flow
369	Q_{svc1}
370	Flow in the upper segment of the superior vena cava (jugular confluence)
371	Q_{svc2}
372	Flow in the lower segment of the superior vena cava
373	Q_{tot}
374	Total inflow
375	Q_{totout}
376	Total outflow
377	Q_{vv}
378	Total flow in the vertebral veins
379	Q_{vvl}
380	Flow in the left vertebral vein
381	Q_{vvr}
382	Flow in the right vertebral vein
383	R_0
384	Resistance to the cerebrospinal fluid outflow
385	R_f

386	Resistance to the cerebrospinal fluid formation
387	
388	ρ
389	Blood density
390	R_{la}
391	Resistance of the basal intracranial arteries
392	R_{pa}
393	Resistance of the pial arterioles
394	R_{pv}
395	Resistance of the proximal intracranial veins
396	R_{vs}
397	Resistance of the terminal intracranial veins
398	R_{vs1}
399	Terminal intracranial vein resistance when P_{ic} is equal to P_{vs}
400	t
401	Time
402	τ_{aut}
403	Time constant of the autoregulation mechanism related to cerebral flow variations
404	τ_{CO_2}
405	Time constant related to CO_2 reactivity
406	VV
407	Vertebral vein
408	x
409	Generic segment of the circuit
410	x_{aut}
411	State variable of the autoregulation mechanism related to cerebral flow variations
412	x_{CO_2}
413	State variable of the autoregulation mechanism related to CO_2

414 **Materials and Methods**

415 **Model description**

416 Our mathematical model for the simulation of the head and cerebral circulation and
417 drainage system includes two submodels built using lumped parameter method. The
418 model is represented in Figure 1.

419
420 (Figure 1)

421
422 Mathematical models may represent an useful tool for improving comprehension of
423 complex systems like this, describing the behavior of a real process using a system of
424 equations [13] [18] [20]. What we are developing is a lumped parameter model, i.e. a
425 model in which the continuous variation in space of the state variables of the system is
426 represented by a finite number of variables [32]. In other words, a lumped parameter
427 model allows the description of spatially distributed physical systems to be simpli-
428 fied using a network of discrete entities that approximate the real system. The use of a
429 lumped parameter model presents a significant advantage since it exhibits a small num-
430 ber of parameters able to account for an entire physiological or clinical phenomenon
431 in a concise way. This fact improves the clinical meaning of the results obtained: the
432 behavior of the model can be studied easily than the system that it represents.

433 Every segment x of Figure 1 consists of a capacitor C_x that simulates the property of
434 the segment to accomodate volume and of a conductance G_x .

435 All the model equations are presented in the Appendix.

436 The mathematical model of the cerebral hemodynamics (enclosed in the "BRAIN"
437 dashed rectangle of Figure 1 has been fully developed and validated by Ursino et al. in
438 previous works [12] [29] [30]. This model simulates the hemodynamics of the arterial-
439 arteriolar and venous cerebrovascular bed, the cerebral arterioles regulation mecha-
440 nisms, the cerebrospinal fluid production and reabsorption processes, the Starling re-
441 sistor mechanism for the cerebral veins and the nonlinear pressure-volume relationship

442 of the craniospinal compartment.
 443 The structure of the cerebral venous outflow model (shown in Figure 1 out of the
 444 "BRAIN" dashed rectangle) has been developed starting from a recent work of Zam-
 445 boni et al. [42]. The main part of the model is composed of 4 venous ducts: 2 internal
 446 jugular veins IJVs (left and right) and 2 vertebral veins VVs (left and right). The inter-
 447 nal jugular veins are modelled by dividing them into 3 segments with different conduc-
 448 tive and capacitive values, to better implement the different biomechanical properties
 449 of these vessels along their length, and to better simulate the effect of hydrostatic pres-
 450 sure gradient in the upright position.
 451 Indeed, jugular veins are collapsible blood vessels characterized by marked changes
 452 in their cross-sectional configuration depending on transmural pressure $P_{xint} - P_{xext}$
 453 [24]. The latter is affected by hydrostatic pressure gradient during a posture change
 454 [6]. On the other side, the hydrostatic pressure gradient does not significantly affect
 455 the lumen of the vertebral veins.
 456 Anatomically speaking, left and right lower jugular segments (J1) correpond to the
 457 segments close to the junction of the IJVs with the subclavian vein, at the confluence
 458 with the brachiocephalic vein trunk. The middle segments (J2) correspond to the point
 459 where the veins are in an anatomical relationship with the more lateral contour of the
 460 thyroid gland. The upper segments (J3) correspond to the point before the passage
 461 through the jugular foramen into the skull [41].
 462 To account for the growth of blood flow from J3 to J1 [5] [7] [9] [26] [31] [39] [42],
 463 we must take into account that a quota of the head inflow is conveyed into the internal
 464 jugular veins more caudally with respect to the J3 position, through intra and extracra-
 465 nial anastomosis. To account for this experimental evidence the model is developed so
 466 that the two jugular veins are linked by a network of 8 constant conductances and 2
 467 constant capacitors that simulate the presence of collaterals and anastomotic connec-
 468 tions. This collateral network also allows the drainage of the extracranial venous blood,
 469 i.e. of that part of blood coming from the two external arteries to serve the head organs
 470 and tissues out of the braincase [42]. We assume that, in basal supine condition, the

471 anastomotic upper connection $c3$ is latent: blood flows in it only when the posture is
 472 upright or when there is a lack of drainage in one vessel tract, or more than one.
 473 Moreover, a basic submodel of 6 constant conductances and 3 constant capacitors is im-
 474 plemented in the main model to describe the lumbo-azygos system (AZY), that links
 475 jugular and vertebral pathways at the level of superior vena cava [33].
 476 The model is made up of several differential equations. Every equation links together
 477 the elements representative of a specific point x (i.e. pressure P_x , conductance G_x and
 478 capacity C_x) with the elements representative of the other segments of the system, in
 479 order to account for mass preservation and to include effects due to posture changes.
 480 We report here (Equations 1 and 2) examples of the two types of equations used to built
 481 the cerebral venous outflow model.
 482 Equation 1, one of the state equations of the model listed in the Appendix, implements
 483 the mass preservation. We can see how the pressure at a given point ($jr3$ in this exam-
 484 ple) is related to capacity, conductances and drops of pressure.

$$\frac{dP_{jr3}}{dt} = \frac{1}{C_{jr3}} [(P_{vs} - P_{jr3}) G_{jr3} - (P_{jr3} - P_{c3}) G_{cjr3} - (P_{jr3} - P_{jr2}) G_{jr2}] \quad (1)$$

485 To include dynamics due to posture changes from supine to upright in the grav-
 486 ity field, conductances in the jugular veins are modeled using a nonlinear relation
 487 (Equation 2) with switch-like properties so that for negative or low transmural pres-
 488 sure $P_{xint} - P_{xext}$ at a given point x , the related vessel conductance G_x is low, while
 489 for high transmural pressure vessel conductance approaches a maximum value [13].

$$G_x = k_x \left(1 + \left(\frac{2}{\pi} \right) \arctan \left(\frac{P_{xint} - P_{xext}}{A} \right) \right)^2 \quad (2)$$

490 The effect of hydrostatic pressure gradient is hidden in the internal pressure P_{xint} .
 491 The value of this pressure decreases by a factor ρgh during the transition from supine
 492 to standing position. Obviously, the collapse of the upper segment of the jugular veins
 493 (J3) is more pronounced with respect to the lower segments (J1), due to the presence

494 of the height h . We use the superior vena cava as the zero level for the hydrostatic
495 pressure.

496 To solve the whole system of equations we resort to an algorithmic approach. We used
497 the software package Berkeley Madonna (free available version beta 9.0.111 [44]), de-
498 veloped on the Berkeley campus under the sponsorship of National Science Foundation
499 and National Institutes of Health (USA) and widely used in biology and biological en-
500 gineering [10] [14]. The package provides three fixed-stepsize integration methods and
501 two variable-stepsize integration methods. We chose the iterative method Runge-Kutta
502 4 to perform all the computations. The algorithms used by Berkeley Madonna are de-
503 rived from the routine methods published in the series of books *Numerical Recipes*
504 [21].

505

506 **Assignment of basal parameters**

507 We adjusted every parameter value in search of agreement between model simulations
508 and measurements that can be obtained from literature results. Starting from the work
509 on the intracranial circuit already developed by Ursino et al.[29], we moved around sev-
510 eral literature data to choose the right inputs for the jugular-vertebral network, adopt-
511 ing reasonable criteria to determine parameters not available from literature. All the
512 intracranial basal parameters are summarized in Table 1.

513

514

515

516

517

518

519

520

521

Table 1: Basal values of quantities related to the intracranial circuit (supine condition).

Quantity	Value
b_{CO_2}	0.5
C_{pan}	$0.205 \text{ ml mmHg}^{-1}$
ΔC_{pa1}	$2.87 \text{ ml mmHg}^{-1}$
ΔC_{pa2}	$0.164 \text{ ml mmHg}^{-1}$
G_{aut}	3
G_{CO_2}	8
k_{CO_2}	15
k_E	0.077 ml^{-1}
k_R	$13.1 \cdot 10^3 \text{ mmHg}^3 \text{ s ml}^{-1}$
k_{ven}	0.155 ml^{-1}
P_a	100 mmHg
P_{aCO_2}	40 mmHg
P_{aCO_2n}	40 mmHg
P_{icn}	9.5 mmHg
P_{pa}	58.9 mmHg
P_v	14.1 mmHg
P_{v1}	-2.5 mmHg
P_{vs}	6 mmHg
Q_n	12.5 ml s^{-1}
R_0	$526.3 \text{ mmHg s ml}^{-1}$
R_f	$2.38 \cdot 10^3 \text{ mmHg s ml}^{-1}$
R_{la}	$0.6 \text{ mmHg s ml}^{-1}$
R_{pv}	$0.880 \text{ mmHg s ml}^{-1}$
R_{vs1}	$0.366 \text{ mmHg s ml}^{-1}$
T_{aut}	20 s
T_{CO_2}	40 s
x_{aut}	$2.16 \cdot 10^{-4}$
x_{CO_2}	0

Table 2: Basal values of pressures related to the jugular-vertebral circuit (supine condition).

Pressure	Symbol	Value (<i>mmHg</i>)
at the collateral (superior tract)	P_{c3}	6.00
at the right jugular (superior tract)	P_{jr3}	5.85
at the left jugular (superior tract)	P_{jl3}	5.85
at the collateral (middle tract)	P_{c2}	5.85
at the vertebral vein	P_{vv}	5.80
at the right jugular (middle tract)	P_{jr2}	5.70
at the left jugular (middle tract)	P_{jl2}	5.70
at the azygos vein	P_{azy}	5.50
at the superior vena cava (superior tract)	P_{svc1}	5.40
at the superior vena cava (inferior tract)	P_{svc}	5.20
at the right atrium (central venous pressure)	P_{cv}	5.00
external at J3 and J2	P_{ext}	0
external at J1	P_{ext}	-6.50

Typical average values reported in Table 2 are assigned as basal values to the pressure of the superior tract of collateral P_{c3} , of venous sinuses pressure P_{vs} and of central venous pressure P_{cv} [13]. Intermediate basal pressure values (P_{jr3} , P_{jr2} , ecc...) are assigned in order to simulate a homogeneous pressure drop along the whole circuit from the exit of venous sinuses to the vena cava. External pressure P_{ext} to the upper sections of the jugular veins J3 and J2 is set to zero, while at the lower segments J1 is set to the average thoracic pressure during a complete respiratory cycle [16].

Looking at the basal flows shown in Table 3, cerebral blood flow Q is the total blood volume entering the cranial cavity per unit time [43]. At the exit from the skull, it is drained both by jugular and vertebral veins, with the two jugular veins that contribute to drain the main part of blood only in supine position. The flow through left and right external carotid arteries Q_{ex} is set according to the data of Yazici et al. [35] and taking

Table 3: Basal values of flows related to the jugular-vertebral circuit (supine condition).

Flow	Symbol	Value (ml/s)
at the brain (cerebral blood flow)	Q	12.50
at every jugular vein	Q_{jr3} and Q_{jl3}	5.85
at every vertebral vein	Q_{vvr} and Q_{vvl}	0.40
at the external duct (face and neck)	Q_{ex}	5.00
at every anastomotic connection	Q_{cjr3} , Q_{cjl3} , Q_{cjr2} , Q_{cjl2}	1.00
at the middle collateral	Q_{c2}	3.00
at the azygos vein	Q_{azy1}	0.40
at the lumbar vein	Q_{lv}	0.13
at the renal vein	Q_{rv}	0.27

into account the lower cerebral flow reported by these authors (i.e., we assumed the same ratio between the extracranial carotid blood flow and blood flow in the common carotid artery as in [35]). It is also assumed that 40% of this flow is directed to every jugular via the anastomotic connections, while the remaining blood is drained down through the middle collateral. Finally, half of the vertebral flow enters in the azygos vein, while the other half is divided between lumbar vein duct (1/3 of the total) and renal vein duct (2/3 of the total).

Parameters A and k_x in the equations describing the conductance of the jugular veins (Equation 2) have been given in order to address two major requirements:

- in supine position, conductances must assume a constant value in accordance with the linear relationship between drops of pressure and flows and in accordance with the values reported in Tables 2 and 3.
- in upright position, the conductance changes induced by venous collapse (consequence of the hydrostatic pressure gradient) determine a redistribution of blood flow from the jugular veins to the vertebral-azygos complex and the collateral

549 route. These changes have been assigned to simulate typical values of jugular
550 blood flow and vertebral blood flow reported in [31].

551 To complete the determination of basal parameters we need to assign a value to
552 every capacity as reported in Table 4. An approximate value for the capacities has been
553 determined by using the following considerations:

- 554 • capacities in the jugular tracts and in the vertebral veins have been computed
555 from the values of transmural pressures, lengths and areas reported in the lit-
556 erature [31] and assuming a negligible unstressed volume (i.e., we consider an
557 average capacity, quite independent of transmural pressure)
- 558 • capacity of the azygos veins are assumed comparable to the capacity of the ver-
559 tebral veins
- 560 • capacities of the collateral tracts have been computed, in the absence of clear
561 geometrical data, by assuming that they are approximately proportional to the
562 square root of conductances, and using the capacities of the jugular tracts as a
563 reference
- 564 • a small value has been given to the capacity of the venous sinuses, since most of
565 these vessels are surrounded by the dura mater

566 Finally we checked that, with the previous choices, the overall capacity of the ve-
567 nous outflow circulation is close to the value used in Ursino et al. (CITA Ursino and
568 Magosso (2010)) for the capacity of the cerebral venous vascular bed (10.7 ml/mmHg).

569
570
571
572

Table 4: Capacities related to the jugular-vertebral circuit (supine condition).

Capacity	Symbol	Value ($ml\ mmHg^{-1}$)
at the venous sinuses	C_{vs}	0.5
at the right jugular (superior tract)	C_{jr3}	1.0
at the left jugular (superior tract)	C_{jl3}	1.0
at the right jugular (middle tract)	C_{jr2}	2.5
at the left jugular (middle tract)	C_{jl2}	2.5
at the central collateral (superior tract)	C_{c3}	0.7
at the central collateral (middle tract)	C_{c2}	1.4
at the superior vena cava (lower tract)	C_{svc}	20
at the azygos vein	C_{azy}	0.5
at the vertebral vein	C_{vv}	0.5

Results and Discussion

Once we verified that the model, with basal parameter values, can simulate the main blood flow changes from supine to upright position, we performed a sensitivity analysis on some model parameters. We focused our attention on changes in conductances in the venous pathways. Indeed, analysis of the correlation between conductances and posture variation and the subsequent pressures and flows changes might give information about the parameters that have greater impact on intracranial hemodynamics (and then on related disorders). From our particular point of view, analysis of the results before and after the variation of a conductance is meaningful, since it provides information on how the closure of a particular drainage tract affects important physiological parameters, such as venous sinuses pressure P_{vs} (and so intracranial pressure P_{ic} and cerebral circulation) or flows in the jugular and vertebral veins (Q_{svc1} and Q_{vv} respectively). For simplicity, we focused only on the right conductance variations, since analyses on left conductance variations will be symmetrical.

Each conductance under examination was varied from the baseline value, that is representative of physiological condition, to zero value that simulate total absence of drainage from a section of the network; simulations of posture variation were performed in both situations.

Once we performed the sensitivity analysis by setting one conductance to zero, we chose to simulate total and halved occlusions of more than one drainage tract at the same time, following the typical patterns in [37].

[9] [15] [17] [26] [28] [34]

Simulations results of particular interest are shown below.

Simulation with basal parameter values

Figure 2 shows how the model simulates the total amount of jugular flow Q_{j3} and vertebral flow Q_{vv} at the equilibrium in both supine and upright condition. Results are also compared with the experimental mean flows reported in Valdueza et al. [31]. The perfect agreement between simulated supine and upright flows and experimental results means that parameters of the model are well assigned.

(Figure 2)

In Figure 3 we show the behavior of the simulated venous sinuses pressure P_{vs} over time when passing from supine to upright condition. When basal parameters are used our model predicts an increase of 2.68 mmHg (from 6.00 to 8.68 mmHg) with change of posture. It also predicts that P_{vs} needs about 3 seconds to reach the upright equilibrium.

(Figure 3)

In Figure 4 the behavior of the simulated right jugular flow Q_{jr3} and right vertebral flow Q_{vvr} over time is reported in the same conditions of Figure 3. For simplicity, we

615 focus the attention only on the right jugular and vertebral flows, since results on left ves-
 616 sels are symmetrical. Figure 4 shows that our model predicts a strong decrease of the
 617 right jugular flow Q_{jr3} when changing from supine to upright (from 6.07 to 0.68 ml/s).
 618 Conversely, flow at the right vertebral vein Q_{vvr} rises from 0.42 to 1.71 ml/s during
 619 change from supine to upright condition. Figure 4 also shows that upright Q_{jr3} and
 620 Q_{vvr} flows reach their equilibrium with different behaviors.
 621 In these conditions the model is simmetrical, namely the flow through jugular and ver-
 622 tebral veins is equally distributed between left and right vessels. The collateral tract $c3$
 623 is latent in supine position, while in upright it drains the amount of blood that not flows
 624 through jugular or vertebral veins (about 8.2 ml/s).

625 (Figure 4)
 626

627
 628 Figure 5 summarizes amounts of simulated total inflow Q_{tot} , flow to face and neck
 629 Q_{ex} , cerebral blood flow Q , total jugular, vertebral and collateral flows at equilibrium
 630 (Q_{j3} , Q_{j2} , Q_{j1} , Q_{vv} and Q_{c3}) in supine and upright conditions.
 631 We see that Q_{tot} is the sum of Q_{ex} and Q . Moreover, the histogram shows the different
 632 type of drainage the cerebral blood flow Q undergoes in supine and upright position.
 633 These different blood distributions are due to the changes in jugular conductances that
 634 occur when upright position is simulated (Equation 2).
 635 Results can be summarized as follow. Cerebral blood flow Q remains substantially
 636 constant despite the posture change, as a consequence of the action of autoregulatory
 637 mechanisms. In fact, the moderate increase in venous sinuses pressure lies well inside
 638 the autoregulatory range [29]. Blood flow Q_{j3} in the upper portion of the jugular vein
 639 exhibits a dramatic fall in the upright state: most of the cerebral blood flow passes
 640 through the collateral route $c3$. Moreover, blood flow in the vertebral veins Q_{vv} in-
 641 creases by about fourfold. These results agree with those reported in literature [31].
 642 Furthermore, blood flow in the jugular veins progressively increases from J3 to J1,
 643 since part of blood flow is drawn from the collateral route to the jugular tract via the

anastomoses cj3 and cj2 (see Figure 1). The reason is that the last portion of the jugular veins exhibit a less pronounced collapse in the upright condition compared to the first tract, due to a smaller gravitational pressure gradient and due to the effect of the negative intrathoracic pressure.

(Figure 5)

Sensitivity analysis

In order to clarify the role of the main routes involved in cerebral venous outflow, and a possible effect of a pathological alteration, we performed a thorough sensitivity analysis. It consists of two steps:

1. We first interrupted blood flow in a single route by assigning value zero to the corresponding conductance, and checked the effect in steady-state conditions;
2. Then, we simulated four typical pathological alterations already reported in the clinical literature [37], and characterized by a conductance reduction in multiple venous paths.

1. Effect of a single closure

Results are summarized in Figure 6, 7 and 8 with regards to the effect of a single closure on venous sinuses pressure P_{vs} , outflow from the confluence of the two jugular veins Q_{svcl} and vertebral blood flow Q_{vv} . Results show that the cerebral venous outflow system is quite robust in response to a single vessel closure, both in supine and upright conditions. This signifies that interruption of a single path can be quite easily replaced by an alternative route. Pressure P_{vs} at the venous sinuses, the link between intracranial and jugular-vertebral circuit, increases with change of posture from supine to upright in basal conditions (+ 2.68 mmHg) as shown in Figure 6. In supine posture,

total occlusion of right jugular vein ($G_{jr3} = 0$, $G_{jr2} = 0$ and $G_{jr1} = 0$) produces little increases of the value of P_{vs} . Also changes due to occlusions of collateral network and vertebral veins are not appreciable. Conversely, looking at the simulation of upright condition, it is evident that P_{vs} is more influenced by lack of drainage of the collateral network ($G_{c3} = 0$), while all the other kinds of occlusion only affect P_{vs} with little or not appreciable increases.

(Figure 6)

Figure 7 shows that output flow from the confluence of jugular veins Q_{svc1} decreases of about -3.1 ml/s from supine to upright. In supine condition, every kind of occlusion evokes little or negligible changes of this flow. The same situation also occurs in upright.

(Figure 7)

Output flow from the vertebral veins Q_{vv} rises of 2.6 ml/s during change from supine to upright conditions as reported in Figure 8. Little variations from the basal supine value occur when a jugular vein is occluded. Conversely, basal upright flow is quite increased by occlusion of the collateral network ($G_{c3} = 0$) and lowered by occlusion of right vertebral vein ($G_{vvr} = 0$).

(Figure 8)

The most influential closure is found in the collateral circulation: in upright conditions it provokes a further increase in venous sinuses pressure up to approximately 10 mmHg, and also a redistribution of blood flow toward the vertebral-azygos complex. Obstruction of a jugular vein is relevant especially when it occurs close to its terminal part, causing a reduction of jugular outflow down to 11.4 ml/s. Naturally, an

Table 5: Venous sinuses pressures and intracranial pressures at equilibrium in simulation of basal conditions and typical stenotic patterns.

Pressure [<i>mmHg</i>]	Supine					Upright				
	Basal	Pattern A	Pattern B	Pattern C	Pattern D	Basal	Pattern A	Pattern B	Pattern C	Pattern D
P_{vs}	5.98	6.51	16.59	13.22	6.01	8.68	9.57	16.60	13.23	9.14
P_{ic}	9.44	9.51	11.09	9.95	9.44	9.81	9.93	11.10	9.95	9.87

obstruction in a vertebral vein causes a significant decline in vertebral blood flow, with a redistribution toward the jugular and collateral circulations.

2. Multiple occlusions

The effect of multiple occlusions may be much more dramatic. In the following, we will especially analyse the changes in venous sinuses pressure, since this quantity represents a link between the cerebral circulation and the extracranial venous outflow system. We report in Figure 9 a histogram to show how the basal venous sinuses pressure P_{vs} varies when stenotic patterns occur. Together with the simulations of null conductance, we reported also the simulations of the same patterns but with halved conductances.

(Figure 9)

A more complete description can be found in Table 5 and Table 6, that report results concerning blood flows and pressures redistribution due to the different stenotic patterns described in [37], in comparison with the simulation of an healthy distribution.

Pattern A refers to simulation of obstruction of the proximal azygos *azy2*, associated with a closed stenosis of the left internal jugular vein. Pattern B refers to simulation of obstructions of both the internal jugular veins and the proximal azygos. Pattern C refers to simulation of obstructions of both the internal jugular but without stenoses in the azygos system. Finally, pattern D refers to simulation of obstructions in different

Table 6: Flows at equilibrium in simulation of basal conditions and typical stenotic patterns.

	Supine					Upright				
Flow [ml/s]	basal	pattern A	pattern B	pattern C	pattern D	basal	pattern A	pattern B	pattern C	pattern D
Q_{vv}	0.79	0.51	3.86	7.86	0.33	3.39	1.54	3.86	7.87	1.37
Q_{jr3}	5.87	11.14	2.97	2.13	6.08	0.69	1.62	3.06	2.10	1.10
Q_{jl3}	5.87	0.81	2.97	2.13	6.08	0.69	1.32	3.06	2.10	1.10
Q_{jr2}	6.87	12.90	3.02	1.86	7.08	1.92	4.99	3.00	1.84	2.48
Q_{jl2}	6.87	0.88	3.02	1.86	7.08	1.92	1.62	3.00	1.84	2.48
Q_{jr1}	7.86	15.39	0.00	0.00	8.08	6.30	13.38	0.00	0.00	7.24
Q_{jl1}	7.86	0.00	0.00	0.00	8.08	6.30	0.00	0.00	0.00	7.24
Q_{svc1}	15.72	15.39	0.00	0.00	16.16	12.59	13.38	0.00	0.00	14.48
Q_{c1}	0.99	1.57	12.98	9.24	1.01	1.46	2.48	12.97	9.23	1.59
Q_{totout}	17.50	17.47	16.91	17.10	17.50	17.45	17.40	16.91	17.10	17.44

720 tracts of the azygos vein (*azy1* and *azy2*) associated with occlusion of the lumbar vein.
 721 Result show that two particular pathological patterns (i.e. patterns B and C) may have a
 722 strong effect on venous sinuses pressure, which reaches values as high as 13-16 mmHg
 723 both in the supine and upright positions. Such value may have consequences on in-
 724 tracranial pressure, CSF circulation and cerebral tissue. However, this pressure increase
 725 occurs only if the stenotic lesions are very severe (conductances close to zero). Moder-
 726 ate levels of conductance changes, although multiple, cause more acceptable pressure
 727 rises.

728 Conclusions

729 We developed a lumped mathematical model for the study of cerebral venous outflow.
 730 It is a lumped model able to simulate the average blood flows in the main drainage
 731 vessels of the brain.
 732 The two main features of the model are that it accounts for the dependence of the
 733 hydraulic properties of the jugular veins with respect to the gravity field, and that it in-
 734 cludes a validated model for the simulation of the intracranial circulation. That makes

735 it an useful tool for the study of the correlations between extracranial blood redistribu-
 736 tions and changes in the intracranial environment.

737 Our first simulations have been useful for testing the robustness of the system of dif-
 738 ferential equations that builds the model. In this perspective, we performed the first
 739 simulations of the effect of change of posture (from supine to upright) on pressures and
 740 blood flows. We performed both simulations of basal drainage and lack of conductance
 741 of some particular vessel tract.

742 Results show that the model is able to reproduce the average physiologic behavior of
 743 the jugular, vertebral, and cerebral ducts. In fact, jugular flow drops from about 11.7
 744 ml/s to about 1.4 ml/s in the passage from supine to standing. At the same time, ver-
 745 tebral flow increases from 0.8 to 3.4 ml/s, while the cerebral blood flow is always
 746 constant at the average value of 12.5 ml/s. All these values are in good agreement with
 747 literature data. In addition to that, the model is able to give informations about the
 748 average flows in different points of the jugular ducts, so taking into account the amount
 749 of blood coming from the anastomotic connections. Moreover, we can easily use it to
 750 verify how the blood redistribution due to change of posture affects the pressures in
 751 specific points of the system.

752 An useful application of the model is the simulation of typical stenotic patterns occur-
 753 ing in venous disorders, as we report in Table 5 and 6.

754 Among all the simulations performed to check the robustness of the model, we want
 755 to stress the fact that it allows us to easily predict how a single obstruction or a given
 756 stenotic pattern affect the average flows and pressures in all the sections of the sytem. A
 757 well validated model can predict not only how the occurence of stenosis affects blood
 758 redistribution, but also how venous disorders change parameters such as venous sinuses
 759 pressure or intracranial pressure, that are essential for the brain regulation.

760 One future work will be to achieve a larger base of data about extracranial circulation,
 761 to improve the setting of the model.

762 Appendix

763 The intracranial circuit

764 Mathematical equations for intracranial blood dynamics and cerebrospinal fluid circu-
765 lation have been written by imposing the mass preservation principle at all the circuit
766 nodes.

767 In the following, we refer to resistance of a given tract R_x as the inverse of the conduc-
768 tance G_x of the same tract.

769

Mass preservation at the node of pial arterioles pa implies the following equation:

$$\frac{d(P_{pa} - P_{ic})}{dt} = \frac{1}{C_{pa}} \left[\frac{P_a - P_{pa}}{R_{la} + R_{pa}/2} - \frac{P_{pa} - P_c}{R_{pa}/2} - \frac{dC_{pa}}{dt}(P_{pa} - P_{ic}) \right] \quad (3)$$

Capillary pressure P_c is given by:

$$P_c = \left(\frac{P_v}{R_{pv}} + \frac{P_{pa}}{R_{pa}/2} + \frac{P_{ic}}{R_f} \right) / \left(\frac{1}{R_{pv}} + \frac{1}{R_{pa}/2} + \frac{1}{R_f} \right) \quad (4)$$

770 The left term of Equation 3 is the variation of transmural pressure in time at the node
771 of pial arterioles. It depends on the blood flow entering and leaving the node (the first
772 two terms in the brackets at the right side) and on the active changes in arterial capacity
773 C_{pa} over time (the last term in brackets). The value of C_{pa} at the denominator accounts
774 for the ability of the duct to store blood without variations of transmural pressure: the
775 higher the value of C_{pa} the lower the change in pressure over time. All other mass
776 preservation equations have a similar meaning.

777

Mass preservation at the node of cerebral veins vi implies the following equation:

$$\frac{d(P_v - P_{ic})}{dt} = \frac{1}{C_{vi}} \left[\frac{P_c - P_v}{R_{pv}} - \frac{P_v - P_{vs}}{R_{vs}} \right] \quad (5)$$

The relationship between C_{vi} and pressure is given by the following equation:

$$C_{vi} = \frac{1}{k_{ven}(P_v - P_{ic} - P_{v1})} \quad (6)$$

Control mechanisms work at the level of the arteriolar cerebrovascular bed by modifying R_{pa} and C_{pa} . Autoregulation activated by relative changes in cerebral blood flow Q is given by the following equation:

$$\frac{dx_{aut}}{dt} = \left(\frac{1}{\tau_{aut}} \right) \left[-x_{aut} + G_{aut} \left(\frac{Q - Q_n}{Q_n} \right) \right] \quad (7)$$

778 where the minus sign of x_{aut} simulates the fact that a fall in blood flow causes a rapid
 779 dilatation of resistance vessels, whereas a rise in blood pressure causes vasoconstriction.
 780 tion.

781

The existence of maximal limits for the vascular response (total vasodilatation and maximal vasoconstriction) is simulated by a sigmoidal static relationship with upper and lower saturation levels acting on pial arteries capacity C_{pa} , so that:

$$C_{pa} = \frac{\left(C_{pa_n} - \frac{\Delta C_{pa}}{2} \right) + \left(C_{pa_n} + \frac{\Delta C_{pa}}{2} \right) \exp \left[\frac{x_{CO_2} - x_{aut}}{k_{C_{pa}}} \right]}{1 + \exp \left[\frac{x_{CO_2} - x_{aut}}{k_{C_{pa}}} \right]} \quad (8)$$

The sigmoidal curve can not be symmetrical because the increase in blood volume induced by vasodilation is higher than the blood volume decrease induced by vasoconstriction. Hence, two different values must be chosen for the parameter ΔC_{pa} , depending on whether vasodilation or vasoconstriction is considered. We have

$$if \ x_{CO_2} - x_{aut} > 0 \ then \ \Delta C_{pa} = \Delta C_{pa1} \ and \ k_{C_{pa}} = \Delta C_{pa1}/4 \quad (9)$$

for the vasodilation simulation, and

$$if \ x_{CO_2} - x_{aut} < 0 \ then \ \Delta C_{pa} = \Delta C_{pa2} \ and \ k_{C_{pa}} = \Delta C_{pa2}/4 \quad (10)$$

782 for the vasoconstriction simulation.

783

The value of pial arteriolar resistance is given by the formula:

$$R_{pa} = \frac{k_R C_{pa_n}^2}{[(P_{pa} - P_{ic}) C_{pa}]^2} \quad (11)$$

The following equations account for cerebrospinal fluid formation rate q_f and out-flow rate q_0 :

$$Q_f = \frac{P_c - P_{ic}}{R_f} \text{ if } P_c > P_{ic}, \text{ else } Q_f = 0 \quad (12)$$

$$Q_0 = \frac{P_{ic} - P_{vs}}{R_0} \text{ if } P_{ic} > P_{vs}, \text{ else } Q_0 = 0 \quad (13)$$

An expression for the resistance of the terminal intracranial veins R_{vs} is computed as follows:

$$R_{vs} = \frac{P_v - P_{vs}}{P_v - P_{ic}} R_{vs1} \text{ if } P_v > P_{vs}, \text{ else } R_{vs} = R_{vs1} \quad (14)$$

Application of mass preservation at the intracranial volume leads to the following equations:

$$\frac{dP_{ic}}{dt} = \frac{1}{C_{ic}} \left[\frac{d(P_{pa} - P_{ic})}{dt} C_{pa} + \frac{d(P_v - P_{ic})}{dt} C_{vi} + \frac{dC_{pa}}{dt} (P_{pa} - P_{ic}) + Q_f - Q_0 + hbf \right] \quad (15)$$

and:

$$C_{ic} = \frac{1}{k_E P_{ic}} \quad (16)$$

784 This formula states that the variation in time of the intracranial pressure is the result of
 785 several factors. The first and the second term in brackets at the right side of Equation 15
 786 refer to changes in transmural pressure at the level of arterioles and cerebral veins,
 787 the third term refers to change on pial artery capacity, while the other terms refer to
 788 cerebrospinal fluid inflow or outflow. Intracranial capacity C_{ic} at the denominator
 789 accounts for the ability of the skull to store volume.

790 **The jugular-vertebral circuit**

791 Mathematical equations for cerebral venous outflow simulation have been written by
 792 imposing the mass preservation principle at all the circuit nodes.

793

The state equations used to build the jugular-vertebral circuit are the following:

$$\begin{aligned} \frac{dP_{vs}}{dt} = \frac{1}{C_{vs}} & [(P_v - P_{vs}) G_{vs} - (P_{vs} - P_{ic}) G_0 - (P_{vs} - P_{jr3}) G_{jr3} \\ & - (P_{vs} - P_{jl3}) G_{jl3} - (P_{vs} - P_{c3}) G_{c3} - (P_{vs} - P_{vv}) G_{vvl1} \\ & - (P_{vs} - P_{vv}) G_{vvr1}] \end{aligned} \quad (17)$$

$$\frac{dP_{jr3}}{dt} = \frac{1}{C_{jr3}} [(P_{vs} - P_{jr3}) G_{jr3} - (P_{jr3} - P_{c3}) G_{cjr3} - (P_{jr3} - P_{jr2}) G_{jr2}] \quad (18)$$

$$\frac{dP_{jr2}}{dt} = \frac{1}{C_{jr2}} [(P_{jr3} - P_{jr2}) G_{jr2} - (P_{jr2} - P_{c2}) G_{cjr2} - (P_{jr2} - P_{svc1}) G_{jr1}] \quad (19)$$

$$\frac{dP_{jl3}}{dt} = \frac{1}{C_{jl3}} [(P_{vs} - P_{jl3}) G_{jl3} - (P_{jl3} - P_{c3}) G_{cjl3} - (P_{jl3} - P_{jl2}) G_{jl2}] \quad (20)$$

$$\frac{dP_{jl2}}{dt} = \frac{1}{C_{jl2}} [(P_{jl3} - P_{jl2}) G_{jl2} - (P_{jl2} - P_{c2}) G_{cjl2} - (P_{jl2} - P_{svc1}) G_{jl1}] \quad (21)$$

$$\begin{aligned} \frac{dP_{c3}}{dt} = \frac{1}{C_{c3}} & [(P_{vs} - P_{c3}) G_{c3} + (P_{jr3} - P_{c3}) G_{cjr3} + (P_{jl3} - P_{c3}) G_{cjl3} \\ & + (P_a - P_{c3}) G_{ex} - (P_{c3} - P_{c2}) G_{c2}] \end{aligned} \quad (22)$$

$$\begin{aligned} \frac{dP_{c2}}{dt} = \frac{1}{C_{c2}} & [(P_{c3} - P_{c2}) G_{c2} + (P_{jr2} - P_{c2}) G_{cjr2} + (P_{jl2} - P_{c2}) G_{cjl2} \\ & - (P_{c2} - P_{cv}) G_{c1}] \end{aligned} \quad (23)$$

$$\frac{dP_{svc}}{dt} = \frac{1}{C_{svc}} [(P_{svc1} - P_{svc}) G_{svc1} + (P_{azy} - P_{svc}) G_{azy2} - (P_{svc} - P_{cv}) G_{svc2}] \quad (24)$$

$$\begin{aligned} \frac{dP_{vv}}{dt} = \frac{1}{C_{vv}} & [(P_{vs} - P_{vv}) G_{vvl1} + (P_{vs} - P_{vv}) G_{vvr1} - (P_{vv} - P_{azy}) G_{azy1} \\ & - (P_{vv} - P_{lv}) G_{vv2}] \end{aligned} \quad (25)$$

$$\frac{dP_{azy}}{dt} = \frac{1}{C_{azy}} [(P_{vv} - P_{azy}) G_{azy1} + (P_{lv} - P_{azy}) G_{lv} - (P_{azy} - P_{svc}) G_{azy2}] \quad (26)$$

The equations used to include dynamics due to posture changes from supine to upright in the gravity field are the following:

$$G_{jr3} = k_{jr3} \left(1 + \left(\frac{2}{\pi} \right) \arctan \left(\frac{P_{vs} - P_{j3ext}}{A} \right) \right)^2 \quad (27)$$

$$G_{jl3} = k_{jl3} \left(1 + \left(\frac{2}{\pi} \right) \arctan \left(\frac{P_{vs} - P_{j3ext}}{A} \right) \right)^2 \quad (28)$$

$$G_{jr2} = k_{jr2} \left(1 + \left(\frac{2}{\pi} \right) \arctan \left(\frac{P_{jr3} - P_{j2ext}}{A} \right) \right)^2 \quad (29)$$

$$G_{jl2} = k_{jl2} \left(1 + \left(\frac{2}{\pi} \right) \arctan \left(\frac{P_{jl3} - P_{j2ext}}{A} \right) \right)^2 \quad (30)$$

$$G_{jr1} = k_{jr1} \left(1 + \left(\frac{2}{\pi} \right) \arctan \left(\frac{P_{jr2} - P_{j1ext}}{A} \right) \right)^2 \quad (31)$$

$$G_{jl1} = k_{jl1} \left(1 + \left(\frac{2}{\pi} \right) \arctan \left(\frac{P_{jl2} - P_{j1ext}}{A} \right) \right)^2 \quad (32)$$

794 **Acknowledgements**

795 **Grants**

796 This study was partially supported by the Italian Minister of Education, University and
797 Research (MIUR Programme PRIN 2010-2011), Grant no. 2010XE5L2R.

798 **Disclosures**

799 The authors declare that they have no competing interests.

References

- [1] **Aaslid R, Lindegaard KF, Sorteberg W, Nornes H.** Cerebral autoregulation dynamics in humans. *Stroke*, 20, 1: 45-52, 1989.
- [2] **Alperin N, Lee SH, Sivaramakrishnan A, Hushek SG.** Quantifying the effect of posture on intracranial physiology in humans by MRI flow studies. *J Magn Reson Imaging*, 22, 5: 591-596, 2005.
- [3] **Bassez S, Flaud P, Chauveau M.** Modeling of the deformation of flexible tubes using a single law: application to veins of the lower limb in man. *J Biomech Eng*, 123, 1: 58-65, 2001.
- [4] **Beggs CB.** Venous hemodynamics in neurological disorders: an analytical review with hydrodynamic analysis. *BMC Med*, 11: 142, 2013.
- [5] **Chambers B, Chambers J, Churilov L, Cameron H, Macdonell R.** Internal jugular and vertebral vein volume flow in patients with clinically isolated syndrome or mild multiple sclerosis and healthy controls: results from a prospective sonographer-blinded study. *Phlebology*, 2013.
- [6] **Cirovic S, Walsh C, Frases WD, Gulino A.** The effect of posture and positive pressure breathing on the hemodynamics of the internal jugular vein. *Aviat Space Environ Med*, 74, 2: 125-131, 2003.
- [7] **Doepp F, Paul F, Valdueza JM, Schmierer K, Schreiber SJ.** No cerebrocervical venous congestion in patients with multiple sclerosis. *Ann Neurol*, 68, 2: 173-183, 2010.
- [8] **Epstein HM, Linde HW, Crampton AR, Ciric IS, Eckenhoff JE.** The vertebral venous plexus as a major cerebral venous outflow tract. *Anesthesiology*, 32, 4: 332-337, 1970.
- [9] **Feng W, Utriainen D, Trifan G, Elias S, Sethi S, Hewett J, Haacke EM.** Characteristics of flow through the internal jugular veins at cervical C2/C3 and C5/C6

- 826 levels for multiple sclerosis patients using MR phase contrast imaging. *Neurol*
827 *Res*, 34, 8: 802-809, 2012.
- 828 [10] **Fontecave-Jallon J, Baconnier P.** Berkeley-Madonna implementation of Ikeda's
829 model. *Conf Proc IEEE Eng Med Biol Soc*, 2007: 582-585, 2007.
- 830 [11] **Fung YC.** *Biomechanics. Circulation*. New York: Springer, 1997, p. xx-yy.
- 831 [12] **Giannessi M, Ursino M, Murray WB.** The design of a digital cerebrovascular
832 simulation model for teaching and research. *Anesth Analg*, 107, 6: 1997-2008,
833 2008.
- 834 [13] **Gisolf J, van Lieshout JJ, van Heusden K, Pott F, Stok WJ, Karemaker JM.**
835 Human cerebral venous outflow pathway depends on posture and central venous
836 pressure. *J Physiol (Lond)*, 560, Pt 1: 317-327, 2004.
- 837 [14] **Grabe M, Oster G.** Regulation of organelle acidity. *J Gen Physiol* 117, 4: 329-
838 344, 2001.
- 839 [15] **Karmon Y, Zivadinov R, Weinstock-Guttman B, Marr K, Valnarov V, Dolic**
840 **K, Kennedy CL, Hojnacki D, Carl EM, Hagemeyer J, Hopkins LN, Levy EI,**
841 **Siddiqui AH.** Comparison of intravascular ultrasound with conventional venog-
842 raphy for detection of extracranial venous abnormalities indicative of chronic
843 cerebrospinal venous insufficiency. *J Vasc Interv Radiol*, 24, 10: 1487-1498.e1,
844 2013.
- 845 [16] **Magosso E, Cavalcanti S, Ursino M.** Theoretical analysis of rest and exercise
846 hemodynamics in patients with total cavopulmonary connection. *Am J Physiol*
847 *Heart Circ Physiol* 282, 3: H1018-H1034, 2002.
- 848 [17] **Mancini M, Lanzillo R, Liuzzi R, Di Donato O, Ragucci M, Monti S, Salva-**
849 **tore E, Morra VB, Salvatore M.** Internal jugular vein blood flow in multiple
850 sclerosis patients and matched controls. *PLoS ONE* 9, 3: e92730, 2014.

- 851 [18] **Olufsen MS, Ottesen JT, Tran HT, Ellwein LM, Lipsitz LA, Novak V.** Blood
852 pressure and blood flow variation during postural change from sitting to standing:
853 model development and validation. *J Appl Physiol* 99, 4: 1523-1537, 2005.
- 854 [19] **Paulson OB, Strandgaard S, Edvinsson L.** Cerebral autoregulation. *Cere-*
855 *brovasc Brain Metab Rev* 2, 2: 161-192, 1990.
- 856 [20] **Piechnik SK, Czosnyka M, Harris NG, Minhas PS, Pickard JD.** A model of
857 the cerebral and cerebrospinal fluid circulations to examine asymmetry in cere-
858 brovascular reactivity. *J Cereb Blood Flow Metab* 21, 2: 182-192, 2001.
- 859 [21] **Press WH, Teukolsky SA, Vetterling WT, Flannery BP.** *Numerical Recipes in*
860 *C.* New York: Cambridge University Press, 1992, p. xx-yy.
- 861 [22] **Radak D, Kolar J, Tanaskovic S, Sagic D, Antonic Z, Mitrasinovic A, Babic**
862 **S, Nenezic D, Ilijevski N.** Morphological and haemodynamic abnormalities in
863 the jugular veins of patients with multiple sclerosis. *Phlebology* 27, 4: 168-172,
864 2012.
- 865 [23] **San Millan Ruiz D, Gailloud D, Rufenacht DA, Delavelle J, Henry F, Fasel**
866 **JH.** The craniocervical venous system in relation to cerebral venous drainage.
867 *AJNR Am J Neuroradiol* 23, 9: 1500-1508, 2002.
- 868 [24] **Schaller B.** Physiology of cerebral venous blood flow: from experimental data in
869 animals to normal function in humans. *Brain Res Brain Res Rev* 46, 3: 243-260,
870 2004.
- 871 [25] **Schreiber SJ, Lürtzing F, Götze R, Doepp F, Klingebiel R, Valdueza JM.** Ex-
872 trajugular pathways of human cerebral venous blood drainage assessed by duplex
873 ultrasound. *J Appl Physiol* 94, 5: 1802-1805, 2003.
- 874 [26] **Thibault P, Lewis W, Niblett S.** Objective duplex ultrasound evaluation of the
875 extracranial circulation in multiple sclerosis patients undergoing venoplasty of
876 internal jugular vein stenoses: A pilot study. *Phlebology* : , 2013.

- 877 [27] **Tobinick E, Vega CP.** The cerebrospinal venous system: anatomy, physiology,
878 and clinical implications. *MedGenMed* 8, 1: 53, 2006.
- 879 [28] **Traboulsee AL, Knox KB, Machan L, Zhao Y, Yee I, Rauscher A, Klass D,**
880 **Szkup P, Otani R, Kopriva D, Lala S, Li DK, Sadovnick D.** Prevalence of
881 extracranial venous narrowing on catheter venography in people with multiple
882 sclerosis, their siblings, and unrelated healthy controls: a blinded, case-control
883 study. *Lancet* 383, 9912: 138-145, 2014.
- 884 [29] **Ursino M, Lodi CA.** A simple mathematical model of the interaction between
885 intracranial pressure and cerebral hemodynamics. *J Appl Physiol* 82, 4: 1256-
886 1269, 1997.
- 887 [30] **Ursino M, Ter Minassian A, Lodi CA, Beydon L.** Cerebral hemodynamics dur-
888 ing arterial and CO_2 pressure changes: in vivo prediction by a mathematical
889 model. *Am J Physiol Heart Circ Physiol* 279, 5: H2439-H2455, 2000.
- 890 [31] **Valdúeza JM, von Münster T, Hoffman O, Schreiber S, Einhüpl KM.** Postu-
891 ral dependency of the cerebral venous outflow. *Lancet* 355, 9199: 200-201, 2000.
- 892 [32] **Waite L.** *Biofluid Mechanics in Cardiovascular Systems*. xx: McGraw-Hill, 2006,
893 p. xx-yy.
- 894 [33] **Werner JD, Siskin GP, Mandato K, Englander M, Herr A.** Review of venous
895 anatomy for venographic interpretation in chronic cerebrospinal venous insuffi-
896 ciency. *J Vasc Interv Radiol* 22, 12: 1681-1690, 2011.
- 897 [34] **Veroux P, Giaquinta A, Perricone D, Lupo L, Gentile F, Virgilio C, Car-**
898 **bonaro A, De Pasquale C, Veroux M.** Internal jugular veins out flow in patients
899 with multiple sclerosis:a catheter venography study. *J Vasc Interv Radiol* 24, 12:
900 1790-1797, 2013.

- 901 [35] **Yazici B, Erdoğan B, Tugay A.** Cerebral blood flow measurements of the ex-
 902 tracranial carotid and vertebral arteries with Doppler ultrasonography in healthy
 903 adults. *Diagn Interv Radiol* 11, 4: 195-198, 2005.
- 904 [36] **Zamboni P, Consorti G, Galeotti R, Giancesini S, Menegatti E, Tacconi G,**
 905 **Carinci F.** Venous collateral circulation of the extracranial cerebrospinal outflow
 906 routes. *Curr Neurovasc Res* 6, 3: 204-212, 2009.
- 907 [37] **Zamboni P, Galeotti R, Menegatti E, Malagoni AM, Tacconi G, Dall'Ara**
 908 **S, Bartolomei I, Salvi F.** Chronic cerebrospinal venous insufficiency in patients
 909 with multiple sclerosis. *J Neurol Neurosurg Psychiatr* 80, 4: 392-399, 2009.
- 910 [38] **Zamboni P, Menegatti E, Occhionorelli S, Salvi F.** The controversy on chronic
 911 cerebrospinal venous insufficiency. *Veins and Lymphatics* 2, 2: 43-48, 2013.
- 912 [39] **Zamboni P, Menegatti E, Pomidori L, Morovic S, Taibi A, Malagoni AM,**
 913 **Cogo AL, Gambaccini M.** Does thoracic pump influence the cerebral venous
 914 return?. *J Appl Physiol* 112, 5: 904-910, 2012.
- 915 [40] **Zamboni P, Menegatti E, Weinstock-Guttman B, Schirda C, Cok JL, Malag-**
 916 **oni AM, Hojnacki D, Kennedy C, Carl E, Dwyer MG, Bergsland N, Galeotti**
 917 **R, Hussein S, Bartolomei I, Salvi F, Ramanathan M, Zivadinov R.** CSF dy-
 918 namics and brain volume in multiple sclerosis are associated with extracranial
 919 venous flow anomalies: a pilot study. *Int Angiol* 29, 2: 140-148, 2010.
- 920 [41] **Zamboni P, Morovic S, Menegatti E, Viselner G, Nicolaides AN.** Screen-
 921 ing for chronic cerebrospinal venous insufficiency (CCSVI) using ultrasound-
 922 recommendations for a protocol. *Int Angiol* 30, 6: 571-597, 2011.
- 923 [42] **Zamboni P, Sisini F, Menegatti E, Taibi A, Malagoni AM, Morovic S, Gam-**
 924 **baccini M.** An ultrasound model to calculate the brain blood outflow through
 925 collateral vessels: a pilot study. *BMC Neurol* 13: 81, 2013.

926 [43] **Zaniewski M, Simka M.** Biophysics of venous return from the brain from the
927 perspective of the pathophysiology of chronic cerebrospinal venous insufficiency.
928 *Rev Recent Clin Trials* 7, 2: 88-92, 2012.

929 [44] [http://www.berkeleymadonna.com/jmadonna/jmadrelease.](http://www.berkeleymadonna.com/jmadonna/jmadrelease.html)
930 [html](http://www.berkeleymadonna.com/jmadonna/jmadrelease.html)

931 **Figure Captions**

932 **Figure 1**

933 Scheme of the lumped parameter model for the study of the cerebral venous outflow.
934 The "BRAIN" box represents the intracranial part of the model, already developed in
935 the work of Ursino et al. [29][30][12]. Outside the "BRAIN" box there is the extracra-
936 nial part of the circuit, that has been developed starting from the work of Zamboni et
937 al. [42].

938 **Figure 2**

939 Comparison between literature flow data [31] and model outcome (right).

940 **Figure 3**

941 Venous sinuses pressure (P_{vs}) behavior over time in supine and upright simulations.

942 **Figure 4**

943 Right jugular (Q_{jr3}) and vertebral (Q_{vvr}) flow behavior over time in supine and upright
944 simulations.

945 **Figure 5**

946 Basal flows in supine and upright simulations.

947 **Figure 6**

948 Sensitivity analysis of venous sinuses pressure P_{vs} .

949 **Figure 7**

950 Sensitivity analysis of jugular veins outflow Q_{svc1} .

951 **Figure 8**

952 Sensitivity analysis of vertebral veins outflow Q_{vv} .

953 **Figure 9**

954 Venous sinuses pressure P_{vs} in healthy and stenotic patterns simulation. The black
955 columns represent the simulation of stenotic patterns with halved conductances with
956 respect to the basal values.

957 **Figures**

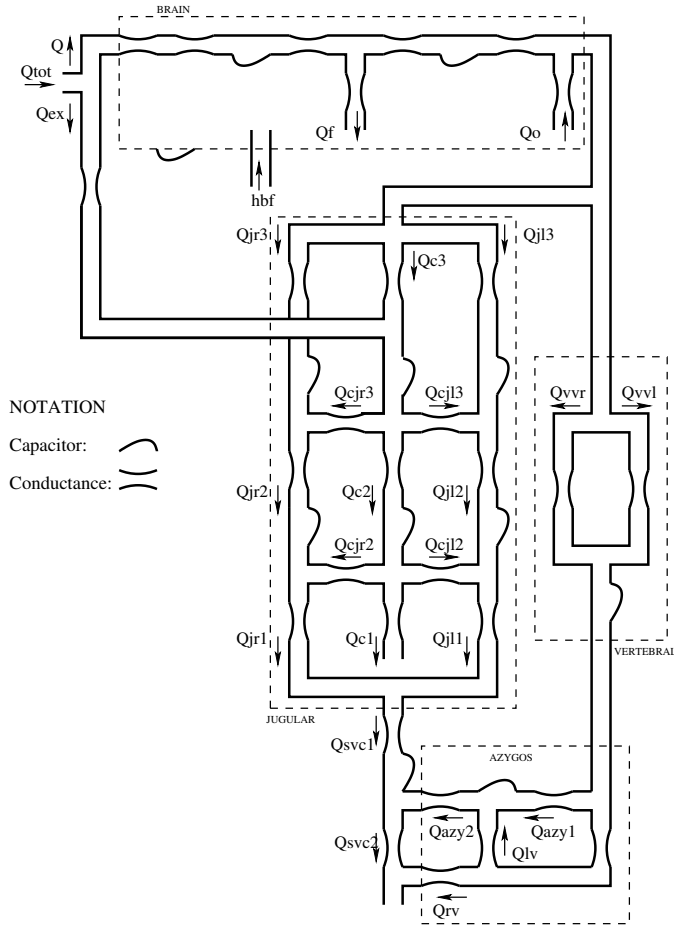


Figure 1: Scheme of the lumped parameter model for the study of the cerebral venous outflow.

The "BRAIN" box represents the intracranial part of the model, already developed in the work of Ursino et al. [29][30][12]. Outside the "BRAIN" box there is the extracranial part of the circuit, that has been developed starting from the work of Zamboni et al. [42].

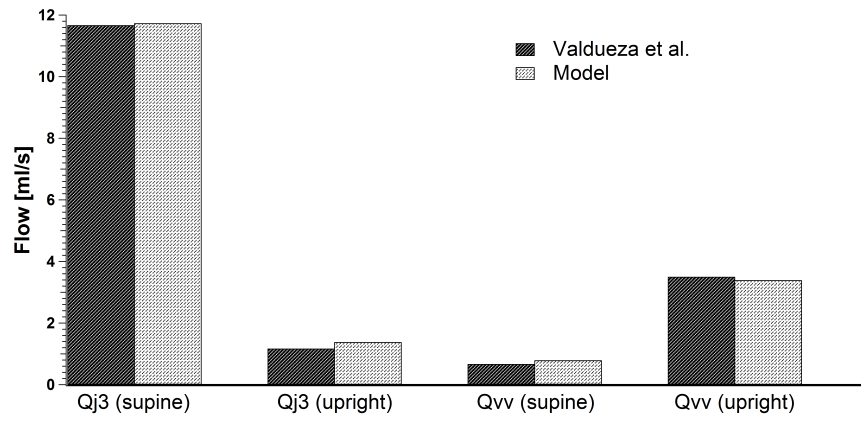


Figure 2: Comparison between literature flow data [31] and model outcome.

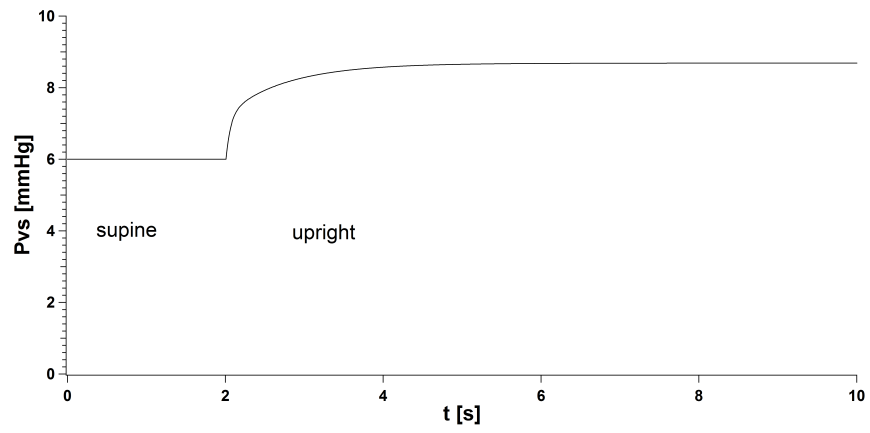


Figure 3: Venous sinuses pressure (P_{vs}) behavior over time in supine and upright simulations.

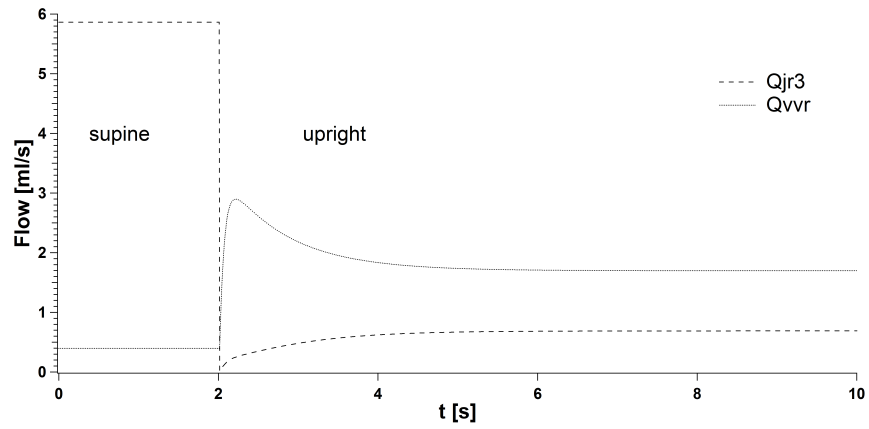


Figure 4: Right jugular (Q_{jr3}) and vertebral (Q_{vvr}) flow behavior over time in supine and upright simulations.

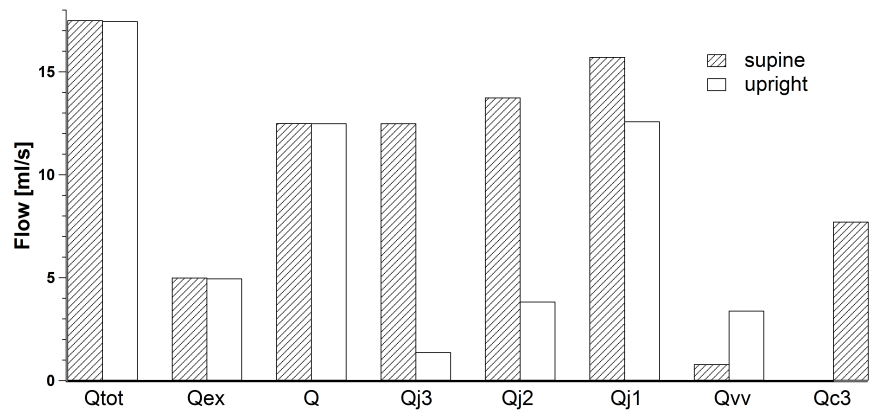


Figure 5: Basal flows in supine and upright simulations.

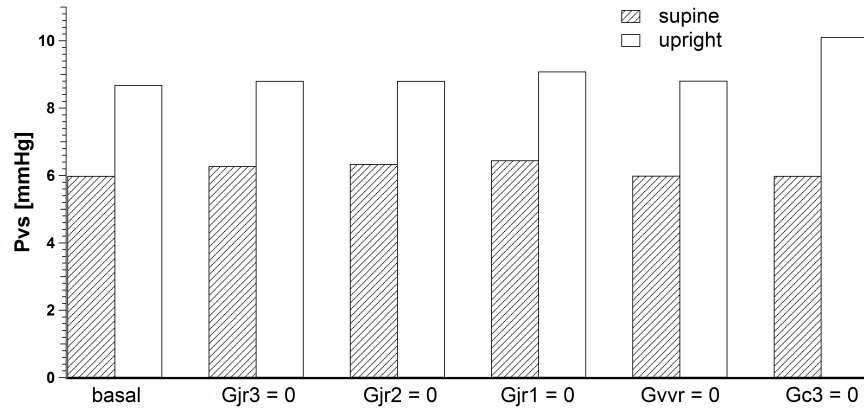


Figure 6: Sensitivity analysis of venous sinuses pressure P_{vs} .

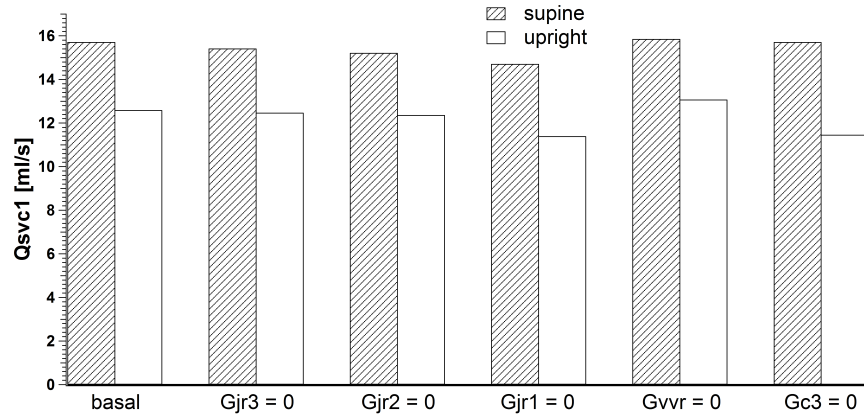


Figure 7: Sensitivity analysis of jugular veins outflow Q_{svc1} .

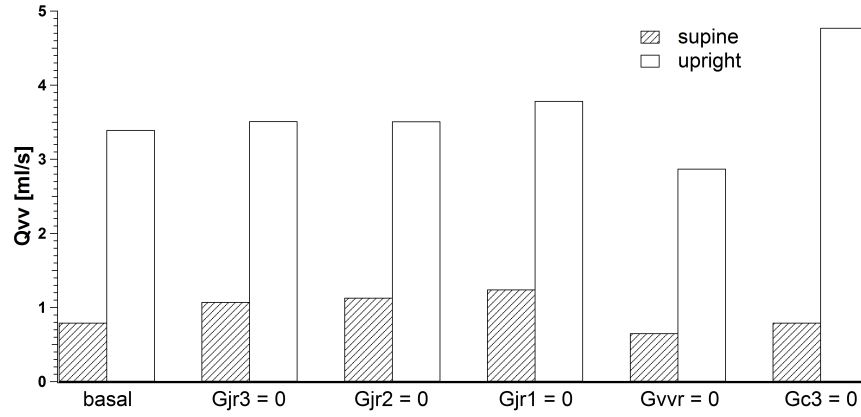


Figure 8: Sensitivity analysis of vertebral veins outflow Q_{vv} .

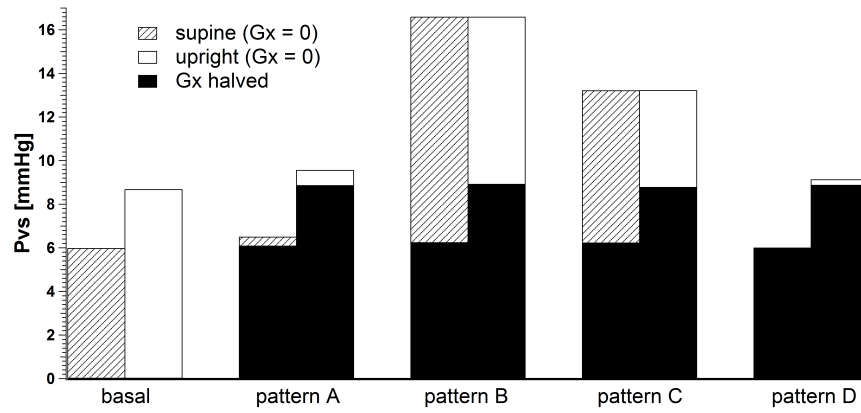


Figure 9: Venous sinuses pressure P_{vs} in healthy and stenotic patterns simulation. The black columns represent the simulation of stenotic patterns with halved conductances with respect to the basal values.